FREE SURFACE MODELING USING CFD:
BUBBLE BURSTING

by

NUR FATIN BTE ALIAS

A project dissertation submitted to the
Chemical Engineering Programme
Universiti Teknologi PETRONAS
in partial fulfilment of the requirement for the
BACHELOR OF ENGINEERING (Hons)
(CHEMICAL ENGINEERING)

UNIVERSITI TEKNOLOGI PETRONAS

TRONOH, PERAK

July 2010

CERTIFICATION OF APPROVAL

Free Surface Modeling by Using CFD: Bubble Bursting

by

Nur Fatin bte Alias

A project dissertation submitted to the

Chemical Engineering Programme

Universiti Teknologi PETRONAS

in partial fulfilment of the requirement for the

BACHELOR OF ENGINEERING (Hons)

(CHEMICAL ENGINEERING)

Approved by,

____

(Dr. Nurul Hasan)

UNIVERSITI TEKNOLOGI PETRONAS

TRONOH, PERAK

July 2010

CERTIFICATION OF ORIGINALITY

This is to certify that I am responsible for the work submitted in this project, that the
original work is my own except as specified in the references and acknowledgements, and that the original work contained herein have not been
undertaken or done by unspecified sources or persons.

NUR FATIN BTE ALIAS

ABSTRACT

Bubble bursting is a process where bubble rises up to a surface of a liquid and experiences bubble film breaks and liquid jet. Invisible to the naked eyes, these two events produce droplets known as film drops and jet drops. There are a lot of industrial problems that are pertinent to these droplets and these problems are very important to be properly handled as they can affect the working environment and workers' health. Realizing the importance of bubble bursting phenomenon, this project has the objective to capture the bubble bursting mechanisms by using CFD and to study the effect of surface tension and initial bubble diameter on bubble bursting mechanism. CFD package that is used in this study is FLUENT 12.0 and the tracking method used is Volume-of-Fluid (VOF). The cases are run for two different surface tension which are 1.2 N/m and 1.4 N/m and two different initial bubble diameter which are 11.5 mm and 9.3 mm. In terms of bubble bursting, the main events of this phenomenon have been captured successfully by CFD where the disintegration of bubble cap and production of liquid jet are observed. However in terms of film and jet droplets formation, this simulation does not show any formation of droplets from the bubble bursting causing no conclusion can be made to relate direct relation between surface tension and initial bubble diameter to the formation of droplets. Improvement can be made to have finer mesh to capture possible formation of droplets in the system.

ACKNOWLEDGMENT

First and foremost, a praise to Almighty for giving me the strength and determination in completing this project. I would like to express my heartfelt gratitude to my supervisor, Dr. Nurul Hasan for his guidance and supports. Without his advice and supervision, this study may not be able to be completed. As a supervisor, he has been a source of motivation towards the completion of this project.

A large measure of gratitude also goes to the following persons who have contributed significantly towards the project:

Dr. Khalik M. Sabil and Dr. Mohanad El-Harbawi, the Final Year Research Project Coordinators, who kindly made the arrangement to provide the students with the necessary tools and materials for research works. Mr. Remy Azuan, the Chemical Engineering Design Laboratory Technician for providing laboratory workspace, apparatus and rendering his technical assistance. Lastly, my sincere thanks to my family for their support and also to friends who not only gave encouragement but also their effort in assisting my project works.

TABLE OF CONTENTS

LIST OF FIGURES

LIST OF TABLES

CHAPTER 1: INTRODUCTION

1.1. Background of Study

It is normal for naked eyes to see the phenomenon as a simple process where bubble rises from the underneath of fluid, and when it reaches the surface, the bubble will burst and disappear. This phenomenon might seem to be insignificant. However, considering bubble bursting phenomenon in industry like metallurgy processes and oceanography, this phenomenon is considered as a critical aspect that seems to be the key point in controlling or improving a process [1].

An application in steelmaking industry that correlates with bubble bursting phenomenon is Electric Furnace Arc (EAF). In EAF, dust formed from the process consists of hazardous metal elements which require specific storage and landfills and the main mechanism of this EAF dust formation is bubble bursting [1]. Similar phenomenon happens in pneumatic steelmaking where bubble bursting is believed to be the source of dust formation [2] and It is proven that the main mechanism of dust formation in pneumatic steelmaking process is the formation of metal droplets that are caused by bubble bursting phenomenon that happened on the free surface of iron melt [3]. These dusts are considerably hazardous as they contained metal oxides, lime, silica, zinc, lead and cadmium. In order to cater the dusts problem, a better understanding of the interaction between the bubble and the system is highly important.

Same goes in electroplating process where bubble bursting phenomenon is causing Cr(VI)-containing droplets which received considerable attention because of high prevalence rates of nasal septum ulcer or perforation among chromium electroplating workers [4]. Furthermore, bubble bursting also is very important in glass-making manufactures as bubbles which formed during the introduction of sand into the molten glass should rise and burst before the glass leaves the furnace [5]. Thus, it might be an interesting attention on how long a bubble will burst, assuming constant surface tension. More interesting, bubble bursting phenomenon also plays an important role in animal cell technology which important in medical product such as viral vaccines, antibodies and human therapeutic proteins, where bubble bursting is implicated as the cause in cell damage in cell culture fermentors [6]. Bubble bursting also can be seen as a mechanism in release of sea salt particles at the ocean surface [7].

From these processes, it can be seen that, a simple phenomenon such as bursting of bubble at a free surface is considerably important to many aspects such as health and hazard risks. Thus, a deep understanding on how this phenomenon occurs, its key parameters and its consequences are highly needed so that, the related industry processes can be improved significantly.

1.2. Problem Statements

A lot of studies have been carried out in investigating bubble bursting phenomenon in order to get clearer view on the related process industries or natural phenomenon. Significant numbers of experiments have been conducted for above objectives. However, an adaption of Computational Fluid Dynamics (CFD) in studying and investigating bubble bursting phenomenon specifically is quite unfamiliar and very few open literature available.

As there are many attempts in solving and modeling bubble bursting phenomenon, with various types of method and approaches, it has to be realized that it is very challenging to model the bubble bursting in terms of computational techniques and computational cost. In this project, bubble bursting phenomenon will be modeled by a chosen CFD package, FLUENT 12.0 to provide significant findings the mechanisms in bubble bursting phenomenon and the effects of key parameters on the bubble bursting.

1.3. Objectives

The objectives of this project are:

1. To simulate bubble bursting mechanisms in a pre-defined condition according to existing experimental studies by using CFD.
2. To validate the numerical solutions with existing experimental results.
3. To redevelop validated mathematical solutions for bubble bursting problem by considering at least two main key parameters, with modeling objective showed in figure below.

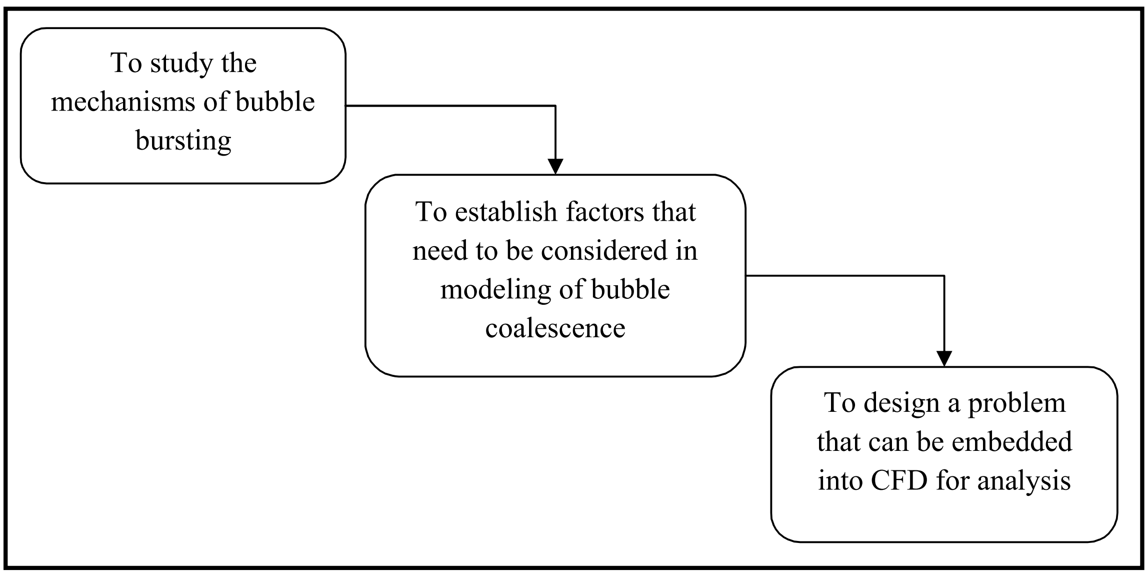

Figure 1.1 Modeling Objectives

1.4. Scope of Study

This paper is expected to fully use the application of a CFD package which is FLUENT 12.0 to investigate the actual mechanisms occurs in bubble bursting and to capture any significant consequences from bubble bursting. In addition, this paper also is expected to examine the effects of two key parameters on the bubble bursting. The key parameters should be depending on the experiments that are going to be used to validate this model and they include surface tension, viscosity and parent bubble diameter. For the computer domain's geometric configuration and all test conditions, they are specified from existing experimental setup. Lastly, the simulation results were compared with the key papers and presented subsequently.

CHAPTER 2: LITERATURE REVIEW

Realizing the importance of bubble bursting towards many industries and applications, numerous studies have been carried out, experimentally and numerically, studying the main situations that occurs during bubble bursting phenomenon. Besides, a lot of existing papers also have studied various key parameters in bubble bursting.

2.1. Validation Papers

Guézennec and colleagues[1] have carried study on bubble bursting phenomenon to capture the formation of film and jet droplets generated from bubble bursting by using high speed camera. They also study the relations between bubble burst phenomenon with generated droplet size and number. They came out with a conclusion on three steps in bubble bursting which produces two types of droplets;

- After the bubble rises and reaches the surface, the bubble floats at the surface with an equilibrium position that can be determined with a thin liquid film that separates the bubble from atmosphere.
- The bubble cap ruptures when the film reaches critical thickness and the disintegration produces fine droplets or film droplets

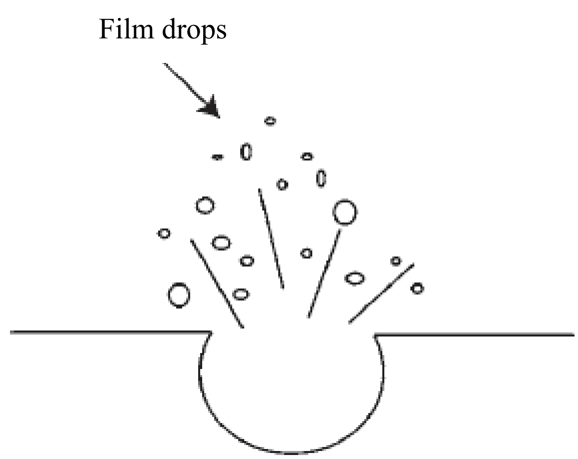

Figure 2.1 Film rupture of a bubble at free surface[1]

- After the rupture, the cavity remaining at the liquid surface closes up, creating an upward jet that is unstable and can break up into droplets which are larger that film droplets. These droplets are called jet droplets.

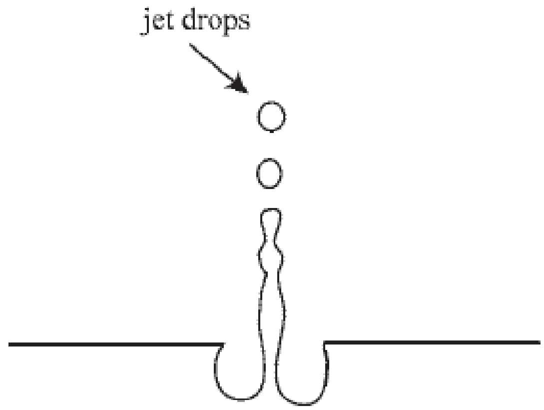

Figure 2.2 Jet drops formation from vertical liquid jet [8]

In this study also, the high speed video proves that the bubble cap ruptures from one point, regardless the bubble size. Experiments carried out by Guézennec and colleagues also showed the jet drop size represents 10 to 18% of the parent bubble size. In this experiment, film drop projections could not be observed in the images due to the limitation on image resolution of the high speed video.

From the study, there are three main aspects that will be replicated in CFD which are:

i. the jet drop size represents 10 to 18 % of parent-bubble size

ii. number of jet drops increases as the parent-bubble decreases, which propose an exponential law;

$$N_{drops} = 43.4\exp(-0.58 d_B) \quad (1)$$

iii. Amount of film drops coming from bubble burst at the surface of the steel bath decreases as the bubble size decreases.

Zhijun Han and Lauri Holappa also had set up an experimental model in investigating the main factors affecting bubble bursting on their paper entitled "Bubble Bursting Phenomenon in Gas/Metal/Slag Systems" [2], where in the paper, they observed bubble bursting phenomenon at the interface of slag/iron systems by using the X-ray transmission techniques and they studied the effects of bubble diameter and surface tension for two cases; bubble bursting on the free surface of molten iron and bubble bursting to the slag/iron interface. They found that the mechanisms of bubble bursting are quite similar to air/water system and two groups of droplet are found in the experiment; fine droplets with diameter few microns up to about 500 μm and bigger droplets with several millimeters in diameter. The fine droplets formed from bubble film cap rupture at the iron melt surface and the bigger droplets are formed from jet produced by collapsing the residual bubble cavity. Figure 2.3 below shows the images that had been captured when bubble bursting occurs.

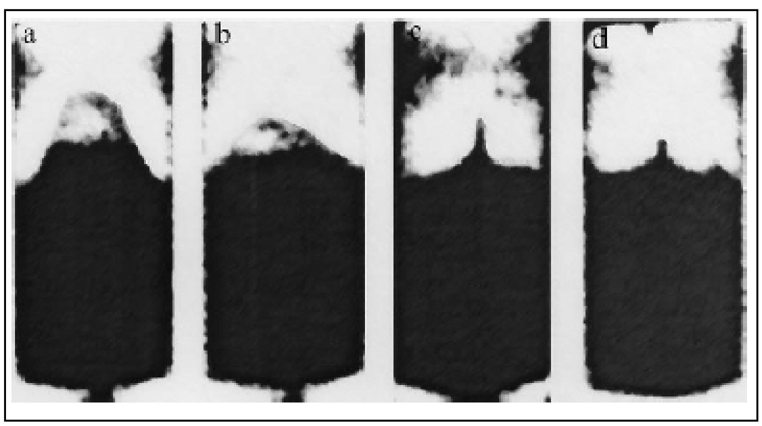

Figure 2.3 X-Ray images of bubble bursting at iron melt surface [2]

Han and Haloppa also showed the relationship between bubble size and surface tension on the formation of droplets from bubble bursting (refer Figure 2.4 and Figure 2.5). These results will be compared to result gained by this paper.

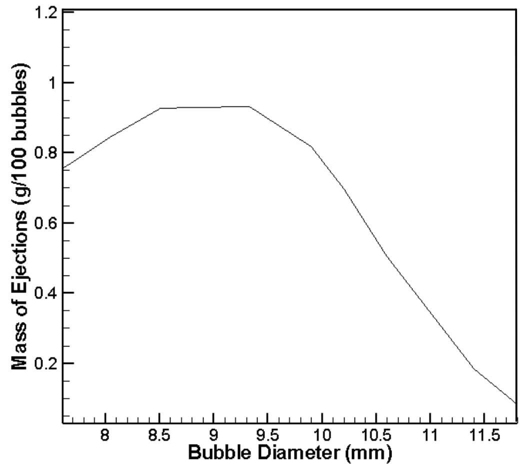

Figure 2.4 Graph of mass of ejection against size of bubble (regenerated)

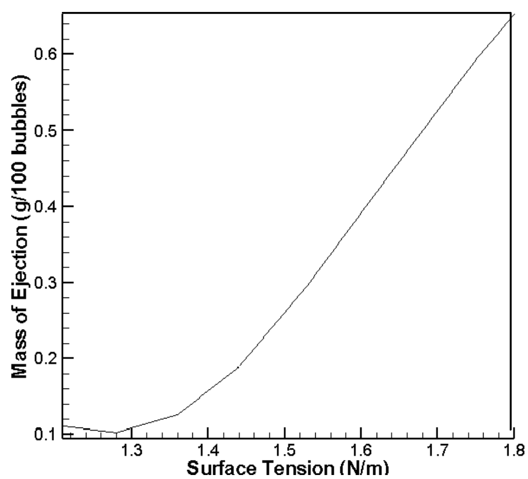

Figure 2.5 Graph of mass of ejection against surface tension for bubble diameter of 11.5mm (regenerated)

Sugimoto and Higayashima [9] also had performed a study on production of water drops due to rupture or air bubbles ate water surface under a positive DC electric field. In a part of their experiment, Sugimoto and Higayashima briefly explained about production of jet drops without electric field, making it similar with other case of bubble bursting. In their study, they showed a linear relationship between size of bubble caps and the diameter of the jet drops released from the water jet. They also observed that size of jet drops are about one-fifth of the film caps. Figure 2.6 below shows the graph that had been developed by Sugimoto and Higayashima.

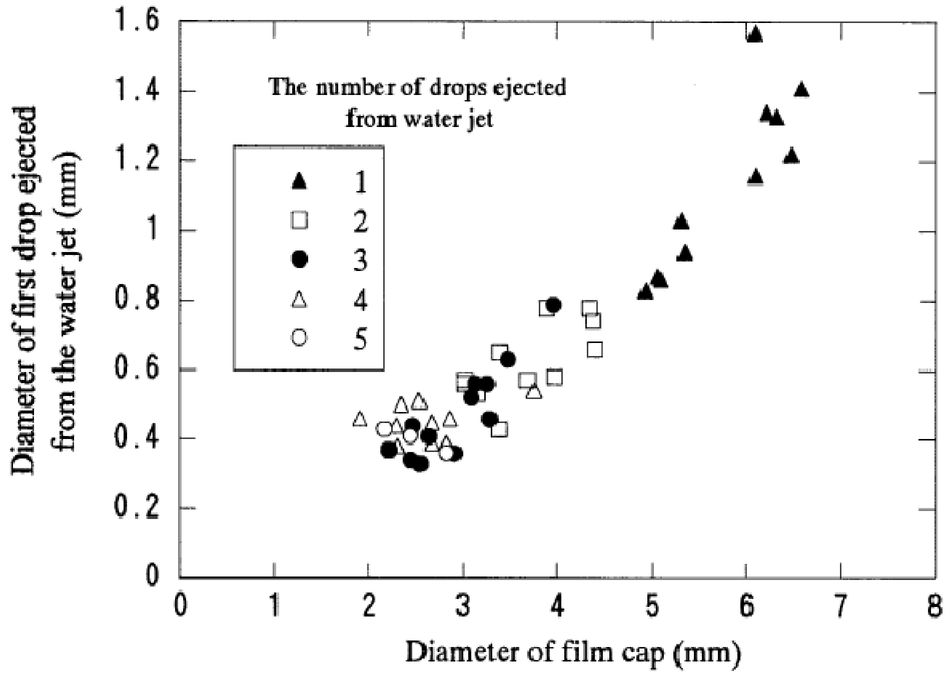

Figure 2.6 Diameter of first drop and number of drops ejected versus diameter of cap [9].

Generally, three papers that have been discussed above is the mother paper or the validation paper that are used by this study. There are a lot more papers and journals that are discussing mainly on bubble bursting phenomenon either experimentally or numerically.

2.2 Other Experimental Studies

Focusing on the droplet generations, Gunther *et al*. [10] investigated the entrainment and transport of film and jet drops from bubble bursting by using Phase Doppler Anemometry (PDA) measurements. In this paper, droplet production was compared between single bubble and multiple bubble or bubbly flow. They managed to found that number of film drops produced from bubble bursting was one order of magnitude larger than the jet drops, the jet drops size increases with parent bubble size and for bubble larger than 4mm in diameter, no jet drops are produced, causing the film droplets to dominate.

2.3 Comparisons between experimental and numerical studies

Boulton-Stone and Blake [11] studied the complex motion occurs when air bubble bursts at air-water interface which resulting in high speed liquid jet. Boulton-Stone and Blake used boundary integral method in modeling numerically the free surface motion and analyze the effect of bubble diameter on bubble bursting. Stone and Blake showed that values of pressure and energy dissipation rates in the fluid indicate a violent motion that causes cell damage in biological industry.

An improvement paper followed, Dey, Boulton-Stone, Emery and Blake have carried out study in explaining the effect of surfactants at free surface to bubble bursting [6]. They compare between experimental data and numerical model, where the study found out the effect of surfactant on time of jet formation, the height and width of jet formed and the number of droplets released. The numerical modeling is based on boundary integral method.

While for Sussman *et al.* [12] they used level set method in capturing the water/air interfaces as boundary integral method is believed to be difficult to be used as bubble bursting phenomenon is consisting merging and breaking up mass of fluid. In Sussman *et al.* [12], fluids are governed by Navier-stokes equation.

Gas bubble bursting process continues to be investigated numerically by Georgescu, Achard and Canot [13]. This numerical solution is using boundary element method with explicit second order time-evolution scheme on several purely Newton fluid and different parent bubble sizes. The fluid flows are governed by Laplace equation for the velocity potential and Euler's equation. Georgescu, Achard and Canot [13] showed similar argument regarding stages in bubble bursting phenomenon with Guézennec *et al.*'s but their model only focusing on jet drop formation, the last stage. The parent bubble sizes used in this study varied from 0.5 mm radius up to critical bubble radius. One of the main findings from this study is when parent bubble size is smaller than critical size, the jets formed split up and produced successive jet drops. However, for parent bubble size greater than critical size, the jet decays without splitting and no jet drops were formed.

CHAPTER 3: METHODOLOGY

This chapter basically explains about the general methodology planned in completing Final Year Project (FYP) for Semester I and Semester 2. This chapter also includes the specific methodology used in achieving the objectives and solving problem statements stated in previous chapter.

3.1. Final Year Project Methodology

Figure3.1 below shows the sequential steps that are planned in achieving the objectives of Final Year Project.

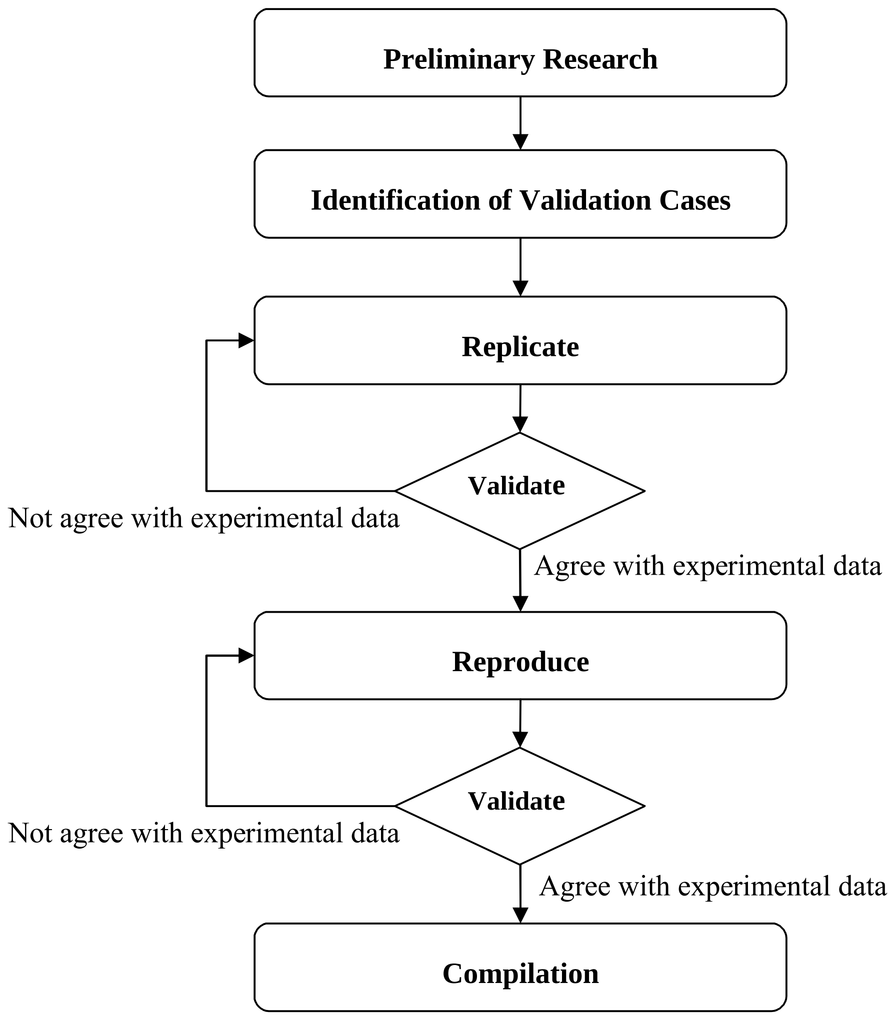

Figure 3.1 Simplified Diagram of Research Methodology in Final Year Project

3.2. Final Year Project Gantt Chart

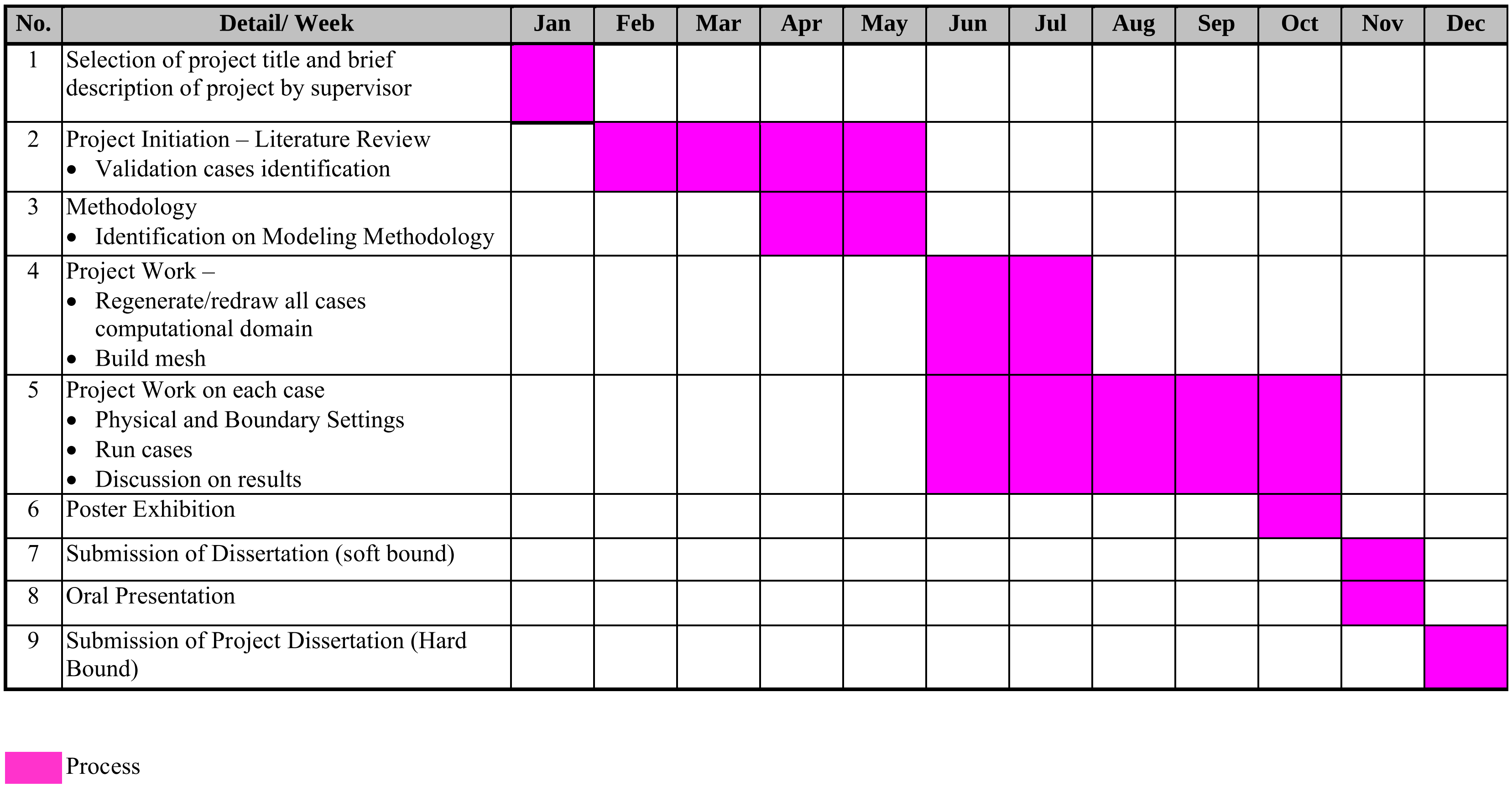

Figure 3.2 Gantt Chart for Final Year Project

3.3. Final Year Project Research Methodology

Preliminary Research includes all activities in gaining basic knowledge and literature reviews on all aspects associated with this study. Basically, there are five main aspects that have been considered to be crucial to be knew in order to have the full grasp about this study. The five aspects are:

- Free Surface Modeling using Computational Dynamics (CFD)
- Volume-of-Fluid (VOF) Method
- Bubble Bursting Phenomenon

All related researches under these five aspects have been discussed in Chapter 2.

In **Identification of Validation Case,** three main cases have been chosen based on the degree of relation with this study. As been mentioned in Chapter Two, the three cases are:

- **Validation Case I**: *Bubble Bursting Phenomenon In Gas/Slag/Metal Systems* by Zhijun Han and Lauri Holappa.
- **Validation Case II**: *Dust Formation By Bubble Burst Phenomenon* by G. Guezennec, J.C. Huber, F. Patisson, Ph. Sessiecq, J.P. Birat and D. Ablitzer.
- **Validation Case III**: *Production of Water Drops and Corona due to Ruptue of Air Bubbles at Water Surface under Positive DC Electric Field* by Toshiyuki Sugimoto and Yoshio Higayashima

In **Replicate** stage, the experimental models in the validation cases will be implemented in FLUENT. All fluid properties, experimental setups, constants and parameters considered in the experiment will be applied in FLUENT. By using FLUENT, the experimental model will be computationally solved and the results will be compared with experimental results from the validation cases. Agreement between computational results and experimental result will validate the computational model used in solving the cases.

3.4. Tools and Equipment

In completing this study, FLUENT 12.0 software is used to study the bubble bursting phenomenon and some modification is done in defining the problem. Prior to FLUENT solving stage, GAMBIT 2.4.6 is used to draw the 3D geometry and generate mesh for problem solving. Most of computational domain related to problems will be drawn by using AutoCAD 2004. For viewing and presenting the results form numerical solution, TECPLOT 360 2010 is used.

3.5. CFD Problem Solving using FLUENT

In applying the experimental models form validation cases in FLUENT, there are steps that are generally carried out in order to achieve the modeling goals. Figure 3.2 below shows the basic procedural steps in solving problems using FLUENT.

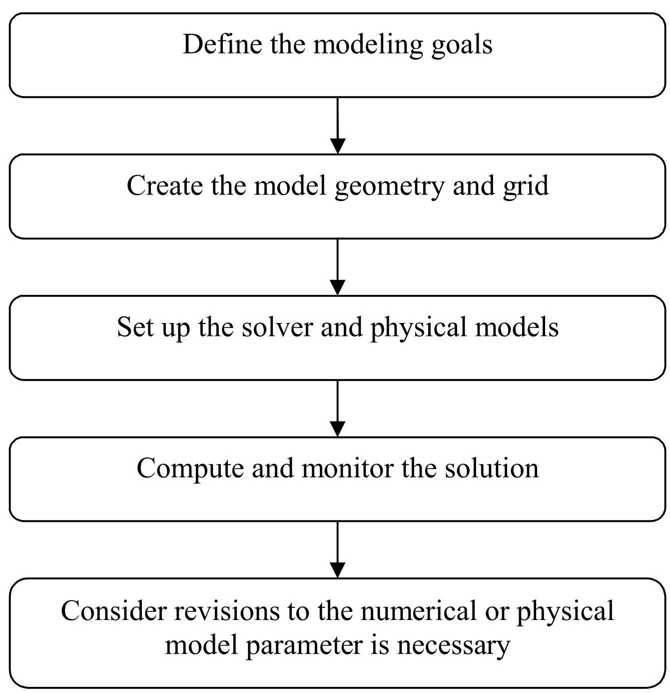

Figure 3.3 Basic procedural steps in solving problem using FLUENT

As the modeling goal has been identified, the Step 2 which is to create the model geometry and grid, FLUENT requires a geometry modeler and grid generator. This study will use GAMBIT Version 2.4.6 as a separate system for geometry modeling and grid generation before it can be solved in FLUENT. The completed geometry and meshes will be solved in FLUENT to get the desired result.

3.6. Overview on Fluid Simulator

3.6.1. <u>Fluid Movement Governing Equation : Navier Stokes Equation</u>

The equations governing the fluid motion are the three fundamental principles of mass, momentum, and energy conservation [14].

Continuity
$$\frac{\partial \rho}{\partial t} + \nabla \cdot (\rho V) = 0 \tag{2}$$

Momentum
$$\rho \frac{DV}{Dt} = \nabla \cdot \tau_{ij} - \nabla p + \rho F = 0 \tag{3}$$

Where ρ of the fluid density, V is the fluid velocity vector, τ_{ij} is the viscous stress tensor, p is pressure, F is the body force, e is the internal energy, Q is the heat source term, t is time, φ is the dissipation term, and ∇.q is the heat loss by conduction.

For incompressible fluid is incompressible and the coefficient of viscosity of the fluid, μ, as well as, coefficient of thermal conductivity are constant, the continuity, momentum, and energy equations reduce to the following equations:

$$\nabla \cdot V = 0 \tag{4}$$

$$\rho \frac{DV}{Dt} = \mu \nabla^2 V - \nabla p + \rho F \tag{5}$$

3.6.2. Interface Tracking Method : Volume of Fluid (VOF)

Volume-of-Fluid is a numerical technique used for tracking and locating the free surface or any fluid-fluid interface. It belongs to the class of Eulerian Methods which are characterized by a mesh that is either stationary moving in a certain prescribed manner to accommodate the evolving shape of the interface. Known for its ability to conserve the mass of traced fluid and when fluid interface changes its topology, this change is traced easily, so the interfaces can join or break apart. The main concept used in VOF is by using fraction function, γ.

γ is defined as the integral of fluid's characteristics function in the control volume or the volume of a computational grid cell.

- When the cell is empty, value of γ would be 0.
- Cell is full; γ =1
- Then the cell consists of fluid-fluid interface, then $0< \gamma <1$

γ is a discontinuous function, its value jumps from 0 to 1 when the argument moves into interior of traced phase. γ also is a scalar function. While the fluid moves with velocity, every fluid particle retains its identity. When a particle is a given phase, it does not change the phase; like a particle of air, that is a part of air bubble in water remains air particle, regardless of the bubble movement.

In bubble/drop volume case [15], considering two phases, without mass exchange and volume averaging the mass and momentum equations, following three cases are encountered as Figure 3.4 below.

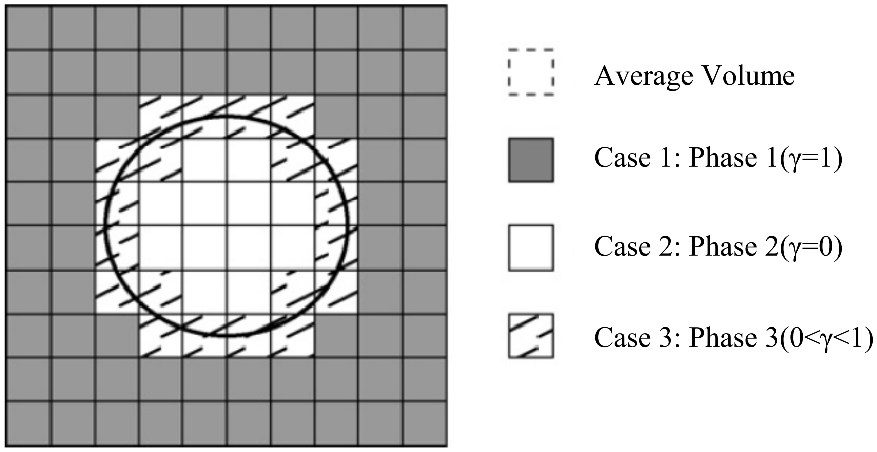

Figure 3.4 Averaging volume compared with bubble/drop volume[15].

Case 1 : The averaging picks out Phase 1

Mass Conservation

$$\frac{\partial\langle\rho_1\rangle}{\partial t}+\nabla\cdot\langle\rho_1 u_1\rangle=0 \tag{6}$$

Momentum Balance

$$\frac{\partial\langle\rho_1 u_1\rangle}{\partial t}+\nabla\cdot\langle\rho_1 u_1 u_1\rangle=\nabla\cdot\langle T_1\rangle+\langle\rho_1 g\rangle \tag{7}$$

Case 2 : The averaging picks out Phase 2

Mass Conservation

$$\frac{\partial\langle\rho_2\rangle}{\partial t}+\nabla\cdot\langle\rho_2 u_2\rangle=0 \tag{8}$$

Momentum Balance

$$\frac{\partial\langle\rho_2 u_2\rangle}{\partial t}+\nabla\cdot\langle\rho_2 u_2 u_2\rangle=\nabla\cdot\langle T_2\rangle+\langle\rho_2 g\rangle \tag{9}$$

Case 3 : The averaging picks out a piece of the interface and both the phases

Mass Conservation

$$\frac{\partial\langle\gamma\rho_1\rangle}{\partial t}+\nabla\cdot\langle\gamma\rho_2 u_2\rangle=0 \tag{10}$$

$$\frac{\partial\langle(1-\gamma)\rho_2\rangle}{\partial t}+\nabla\cdot\langle(1-\gamma)\rho_2 u_2\rangle=0 \tag{11}$$

Momentum Balance

$$\frac{\partial\langle\gamma\rho_1 u_1\rangle}{\partial t}+\nabla\cdot\langle\gamma\rho_1 u_1 u_1\rangle=\nabla\cdot\langle\gamma T_1\rangle+\langle\gamma\rho_1 g\rangle+\frac{1}{V}\int_{AI} T_1\cdot n_{I12}dA \tag{12}$$

$$\frac{\partial\langle(1-\gamma)\rho_2 u_2\rangle}{\partial t}+\nabla\cdot\langle(1-\gamma)\rho_2 u_2 u_2\rangle=$$

$$\nabla\cdot\langle(1-\gamma)T_2\rangle+\langle(1-\gamma)\rho_2 g\rangle+\frac{1}{V}\int_{AI} T_2\cdot n_{I21}dA \tag{13}$$

3.7. Validation Case I: Bubble bursting phenomenon in Gas/Metal/Slag systems

In Bubble Bursting Phenomenon in Gas/Metal/Slag Systems [2], bubble bursting phenomenon had been studied at the surface of molten iron. The main objective of [2] is to study the relationship between surface tension and parent bubble diameter with the mass of ejection from bubble bursting.

3.7.1. Solution Domain Setup

In studying bubble bursting at gas/metal/slag system, Han and Holappa have used X-ray transmission technique as shown in Figure below. The system consists of vertical electrical resistant furnace, X-ray imaging system and a gas supply and control system.

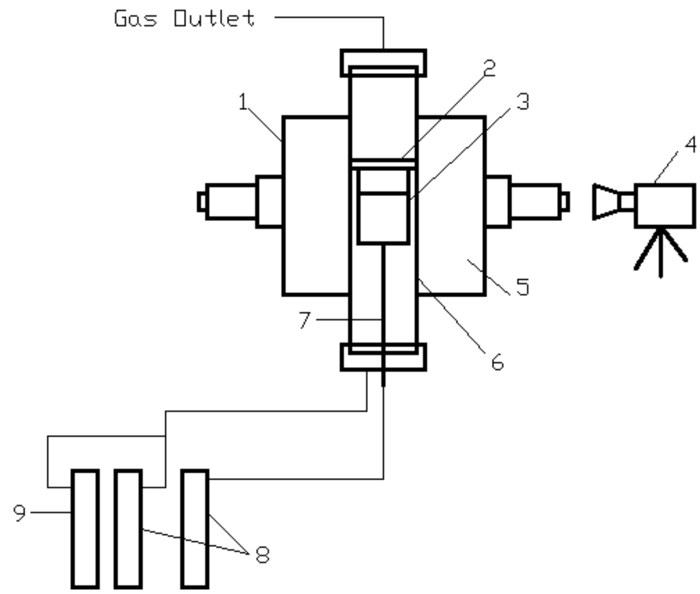

1	Furnace Shell	6	Furnace Tube
2	Ceramic Plate	7	Capillary
3	Crucible	8	Argon Gas
4	CCD Camera	9	10%H_2 + 90% Ar gas
5	Refractory Insulation		

Figure 3.5 Experimental setup for Bubble Bursting Phenomenon in Gas/Metal/Slag System[2].

The images produced by X-ray receiver are captured by a high-resolution CCD camera (Hamamatsu-54505-01) with resolution of 360x575 and the images are recorded in cassette. Bubble bursting occurs in crucible with inner diameter of 30mm and height of 50mm, where in this crucible places 150-g electrolytic iron and alumina plate to collect ejected droplets.

3.7.2. Geometry of Computational Domain

The geometry of the crucible is redrawn as shown in Figure 3.4. The dimensions are set to be similar with experimental setup. This schematic geometry is drawn by using AutoCAD 2004. As dimensions of the crucible are given in the experimental data, the only thing that needs to be calculated is the height of iron melt in the crucible. This height is easily calculated by using given mass and density of iron melt.

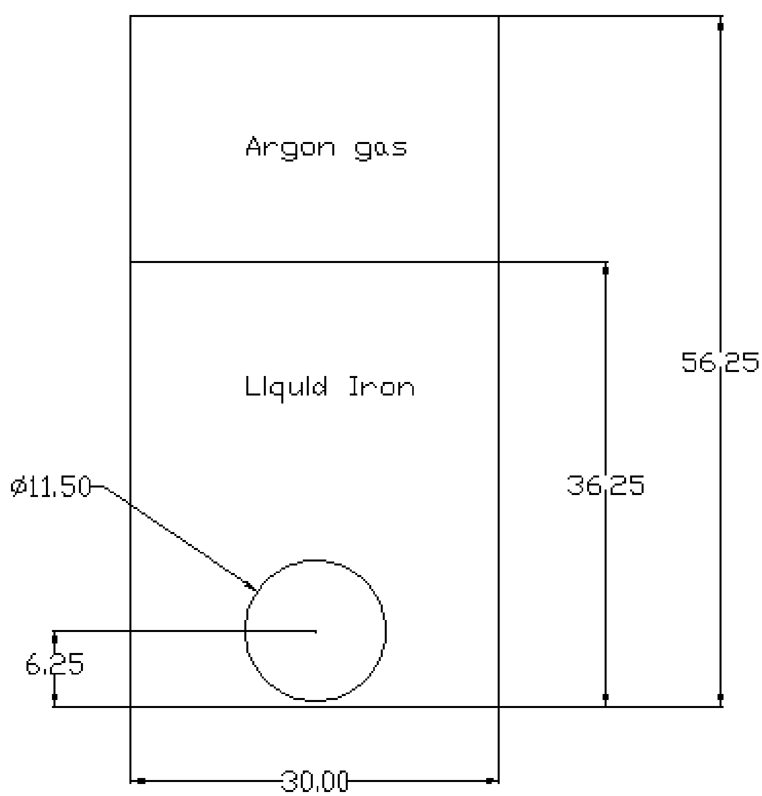

Figure 3.6 Redrawn Experimental setup for Validation Case I (focused in crucible only)

Table 3.1 Geometric Configuration of the Computational Domain for Case I

Argon Bubble Diameter	11.5 mm
Crucible Inner Diameter Height Mass of Electrolytic iron Density of Electrolytic Iron Height of Electrolytic Iron in Crucible	 30 mm 50 mm 150 g 7.1 g/cm^3 30 mm
Surface Tension	1.2 N/m^2
Total Number of Cells	260325

3.7.3. Model and Numerical Background

Simulations were run on a Hewlett-Packard HP xw8400 Workstation with 8.00 GB of RAM by using a chosen CFD package, FLUENT 12.0. This simulation was taken place in 3D space instead of axisymmetric as bubble shape cannot be assumed to be uniform in all axes throughout the time. The solver had been set to be in Pressure-Based as momentum and pressure were going to be the primary variables. Transient or Unsteady time was aligned with real case situation where the process taken place in the experiment was not stable with time. Table 3.2 below summarizes the settings that have been set up in defining the solver.

Table 3.2 Solver Settings used in Validation Case I Simulation

Model Setting	
Solver	Pressure Based
Formulation	Implicit
Space	3D
Time	Unsteady
Velocity Formulation	Absolute
Gradient Option	Green-Gauss Cell Based

For simulations of fluid-fluid interface using a finite volume approach with existence of breakup of interface surface, Volume of Fluid (VOF) Model is very suitable as VOF allows mass conservation [15]. Table 3.3 below summarizes the settings needed for multiphase model.

Table 3.3 Multiphase Settings used in Validation Case I Simulation

Multiphase Model	
Model	Volume of Fluid
Number of Phases	2
VOF Scheme	Explicit
Courant Number	0.25
Open Channel Flow	Disable
Implicit Body Force	Disable

This simulation is set to cover the bubble bursting phenomenon for approximately 0.01 real seconds as bubble bursting phenomenon is a very quick process as break up of bubble cap is expected to be about 0.05 real seconds [16]. Table 3.4 below summarizes the settings that are being used in time step solver.

Table 3.4 Time Solver Setting for Validation Case I Simulation

Iterate : Time	
Time Step Size	0.0001s
Number of Time Steps	100
Time Stepping Method	Fixed
Max Iterations per Time Step	100
Autosave Data	Data File Every 10 time steps

Generally, simulation settings for all three validation cases are expected to be similar except in Material Selections, Computational Domain and Dimensions and Physical Properties such as Surface Tension and Viscosity.

3.8. Validation Case II: Dust formation in Electric Arc Furnace

Dust Formation in Electric Arc Furnace [1] is quite similar to be compared with Bubble Bursting Phenomenon in Gas/Metal/Slag System [2]. Their obvious difference is regarding the dimensions of the crucible and size of parent bubble.

3.8.1. Experimental and Simulation Setup

The original experimental setup consist a vacuum induction melting furnace which had been modified to operate at atmospheric pressure under an argon atmosphere (refer to Figure 3.5). The difference between this case and the previous case mainly are on the the dimensions of the equipments and the initial size of the bubble.

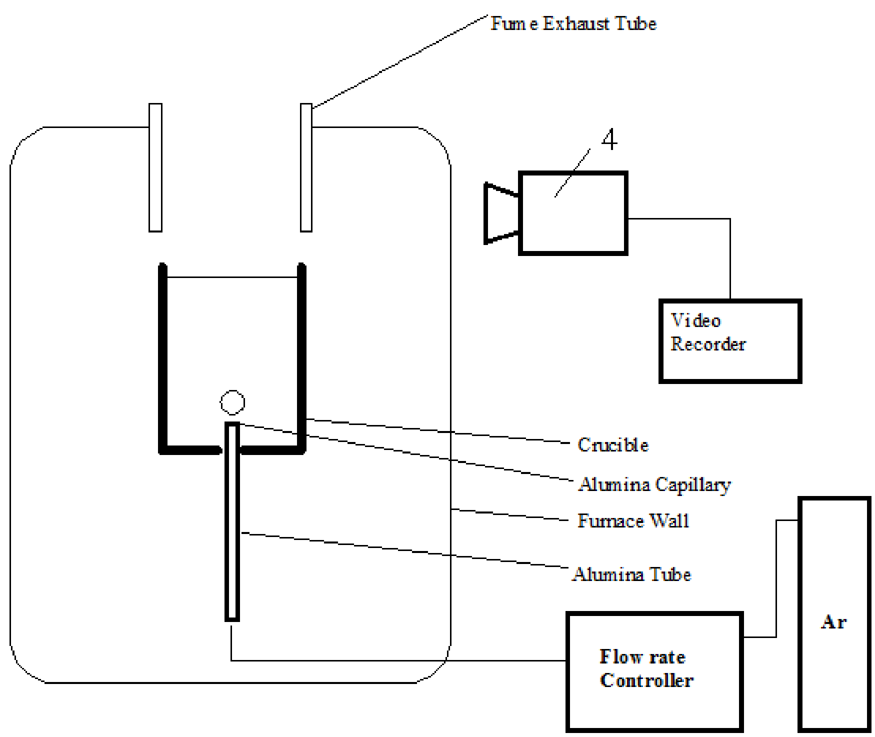

Figure 3.7 Experimental Setup done by Guezennec et. al.[1]

3.8.2. Geometry and Grid

For this case, the focus is inside the crucible which contains 750g of commercial steel grade. This crucible is in 45mm inside diameter and 70mm height and the geometry of the crucible is redrawn as shown in Figure 3.8. The dimensions are set to be similar with experimental setup. This schematic geometry is drawn by using AutoCAD 2004. As dimensions of the crucible are given in the experimental

Figure 3.8 shows the location of bubble which is located at the bottom of the crucible. In this example, the diameter of bubble is 7 mm. Depending on different cases, the diameter of bubble is changing.

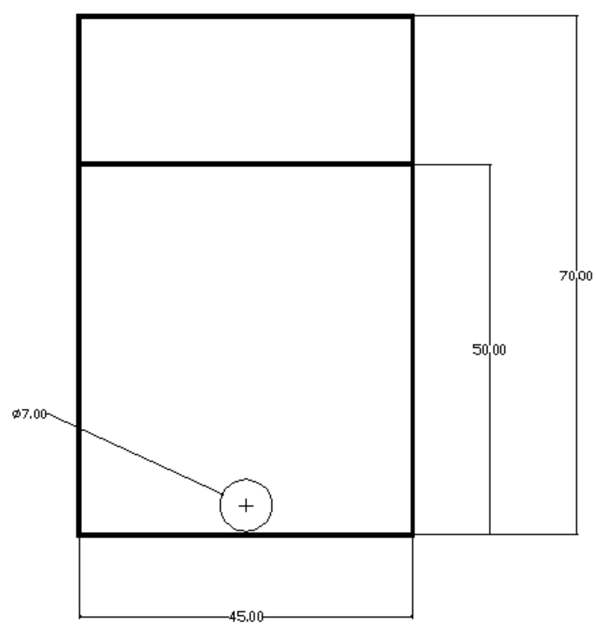

Figure 3.8 Details on crucible used by Guezzenec et al. [1]

3.8.3. Model and Numerical Background

Simulations were run on a Hewlett-Packard HP xw8400 Workstation with 8.00 GB of RAM by using a chosen CFD package, FLUENT 12.0. This simulation was taken place in 3D space instead of axisymmetric as bubble shape is not uniform throughout the time. The solver had been set to be in Pressure-Based as momentum and pressure were going to be the primary variables. Transient or Unsteady time was aligned with real case situation where the process taken place in the experiment was not stable with time. The basic simulation settings are set similar to Validation Case I. Based on same materials, the surface tension also is kept same with Validation Case I. Validation Case II is different in terms of size of bubble and dimensions of crucible.

3.9. Validation Case III: Production of Water Drops and Corona due to Rupture of Air Bubbles at Water Surface under a Positive DC Electric Field

In Case III [9], the study is regarding bubble bursting phenomenon at water surface under a positive DC electric field. However, there is an earlier part where Sugimoto and Higayashima run the case without electric field. This part has been chosen to be a validation case to be compared with simulation results.

3.9.1. Experimental and Simulation Setup

The original experimental setup consist a water vessel containing tap water which is surrounded with thermal insulation. Air bubbles are produced from silicon tube which is having diameter of 0.4 mm. The dimension of the water vessel is 100mm x 100mm x 100mm. Relatively to bubble diameter of 2.8 mm, the dimension of the water vessel is considered large and reconstructing the large domain in the simulator will require high computational cost and longer time to solve. It is then decided for Case III to have the same geometrical domain except the initial bubble size.

3.9.2. Model and Numerical Background

The model and numerical background for Validation Case III is set to be similar with Case I and Case III.

CHAPTER 4: RESULTS AND DISCUSSIONS

4.1. Bubble Bursting Phenomenon

To capture bubble bursting phenomenon by using CFD is one of the main objectives of this project. Based on the collected result, it can be seen that bubble bursting phenomenon that is captured by using FLUENT 12.0 is quite similar with the literature review. In describing the phenomenon of bubble bursting, below case is for bubble diameter of 11.5 mm and 0.5 N/m^2 of surface tension. Details are explained in paragraph below. Bubble bursting phenomenon is divided into two main events which are bubble film breakage and liquid jet production.

4.1.1. Bubble Film Breakage

As the bubble rises from liquid and meets the surface, it curves the surface for a hemisphere-looked like shape (refer Figure 4.1). The liquid film forms and separates the bubble from the atmosphere. In simulation, the rising of bubble from the bottom of the tank is calculated with step size of 0.001s. It appears the time taken for the bubble to arrive at the surface which located 30mm from the initial point of the bubble, is approximately 0.1s.

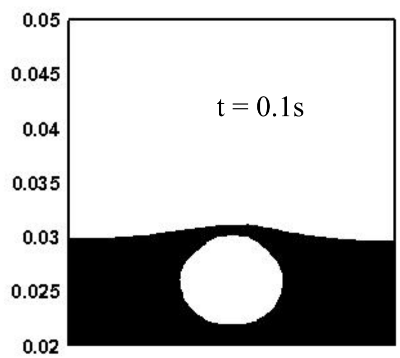

Figure 4.1 Bubble at liquid surface before burst

Having its equilibrium position, the bubble can rest for a certain period of time while the liquid film is drained until the film reaches its critical thickness before it bursts. The equilibrium position of the bubble at atmosphere had been studied by Georgescu[13]. During its equilibrium position, the liquid film is drained and the film becomes thin eventually. The film is thin enough for inter-molecular forces to take over before the film rapidly ruptures. The film rupture begins from one point which looked like a hole. This point can be anywhere on the bubble cap.

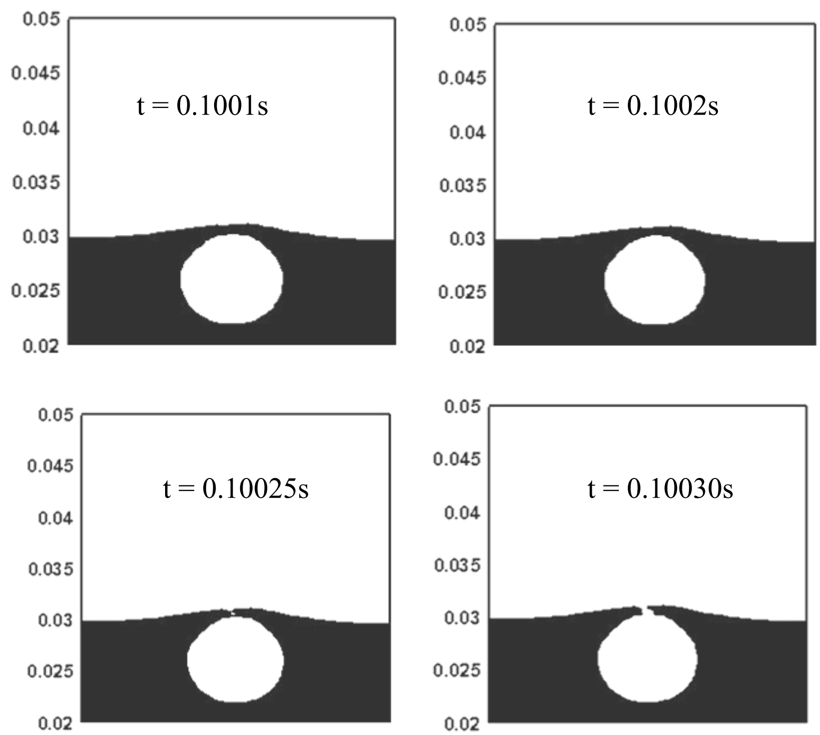

Figure 4.2 Single point breaks on bubble cap

It can be observed above that one point of breakage exists on the bubble cap, merely at the center of the cap on 0.10025s. It means, the bubble rests on the surface, having its liquid film drained until its critical thickness and start to burst 0.25 ms after the bubble reaches the surface. In order to justify other phenomenon occur in bubble bursting, this point is taken as a reference point. Bubble burst is started when the single point of hole occur on bubble cap.

To compare with existing literature review, Guezennec et. al [1] had shown that bubble film disintegration is started with formation of a hole on the bubble film at 0.2ms after the bubble reach its equilibrium position on liquid surface.

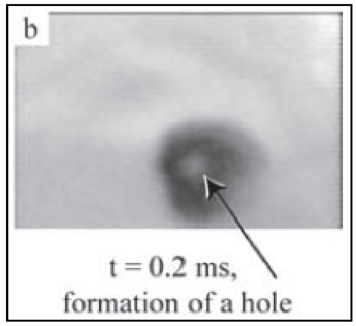

Figure 4.3 Formation of hole during bubble film breakage[1]

From this point, the hole widens or can be known as disintegration of bubble cap into fine droplets or film drops, until the film disappeared. Studies had been conducted extensively regarding the relationship between number and size of film drops depending on size of parent bubble.

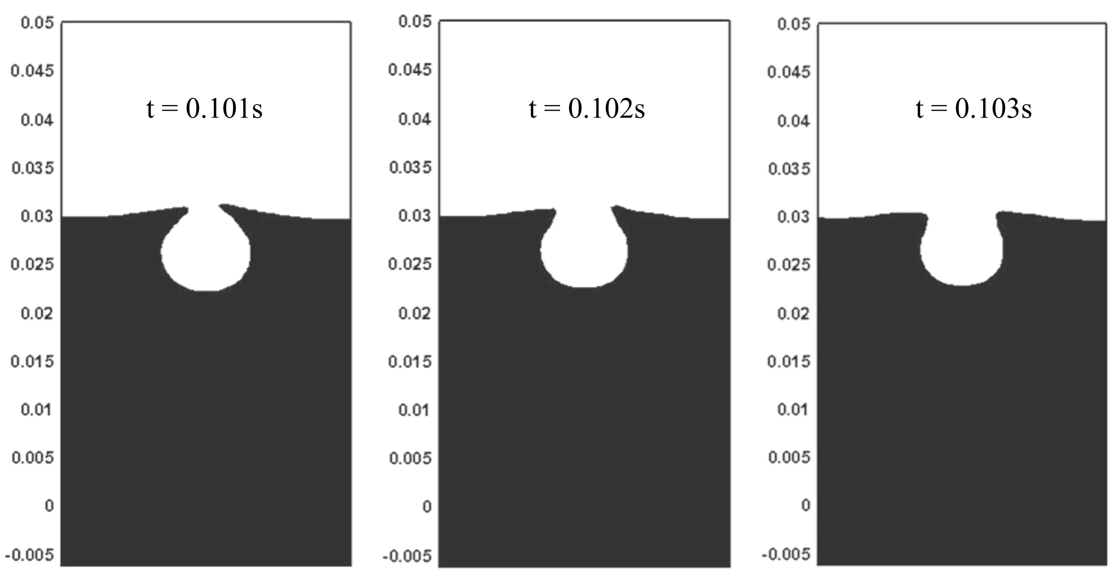

Figure 4.4 Disintegration of bubble cap

Figure 4.4 shows how the initial hole that exists on the cap widens and it took approximately 0.002 sec for the cap to completely disappear.

The expectation of bubble film disintegration is the formation of film droplets. These droplets' size range up from few micron to 500µm[2]. In this simulation, the results do not show any formation of bubble film droplets. This might be due to coarse mesh that does not fine enough to capture fine droplets.

4.1.2. Liquid Jet Production

After the disruption of bubble cap, there is cavity remaining at the liquid surface which tends to close up and creating an upward liquid jet (refer Figure 4.5).

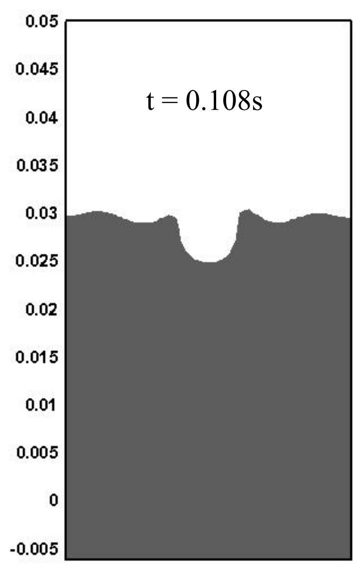

Figure 4.5 Liquid surface tends to close up to produce liquid jet

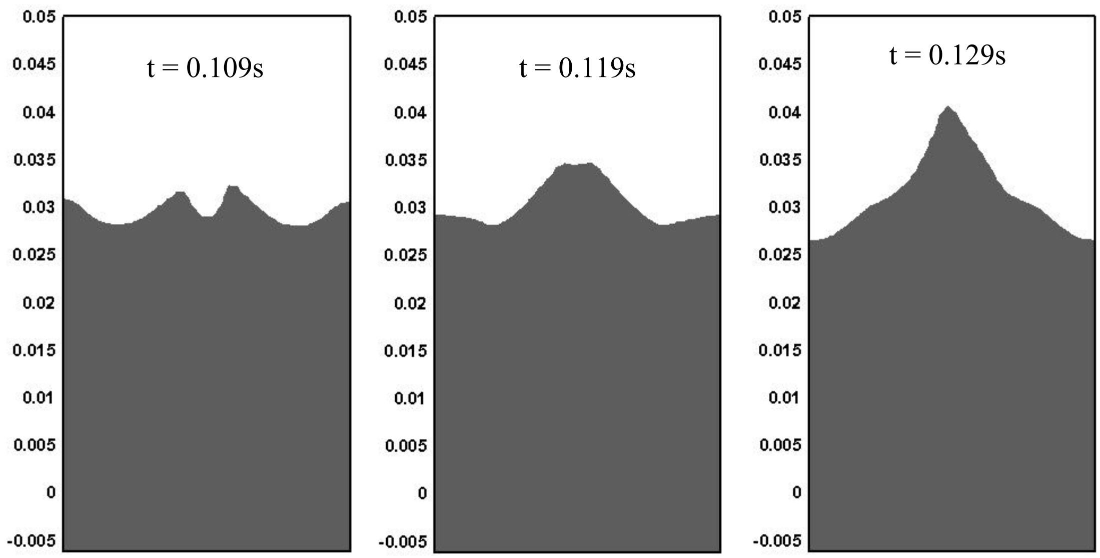

Figure 4.6 Liquid Jet Production

From Figure 4.6, it can be seen that liquid jet is produced with height of 16 mm from the liquid surface. Liquid jet that produced is unstable and can disintegrate to produce droplets. This result is expected to produce jet droplets that could be disintegrated from the liquid jet. However, there is none droplets that can be seen. This result might be due to coarse mesh or the bubble diameter is larger than critical bubble diameter in iron/argon system that is yet to be determined.

Jet production is influenced by the size of bubble. In explaining the effect of bubble size to jet production, bubble size is divided into two kinds; bigger than critical size, and smaller than critical size. For a bubble with critical size, the submerged and protruding portion is equally distributed, forming an almost hemispherical shape of the submerged portion. For bubble which sized smaller than the critical size, the protruding smaller is smaller than the submerged, where the center of curvature of bubble cavity is below the free surface. While for bigger bubble, the submerged is smaller compared to the protruding portion. The deeper the centre of curvature of bubble, the harder the energetic jet will be. This would explain about no jet droplets will be produced for bubble bigger than critical size.

4.1.3. Comparison with Literature Review

This comparison is made focusing only on bubble bursting phenomenon. Figure 4.5 below is the results that are gathered by Sugimoto and Higayashima in their paper[9].

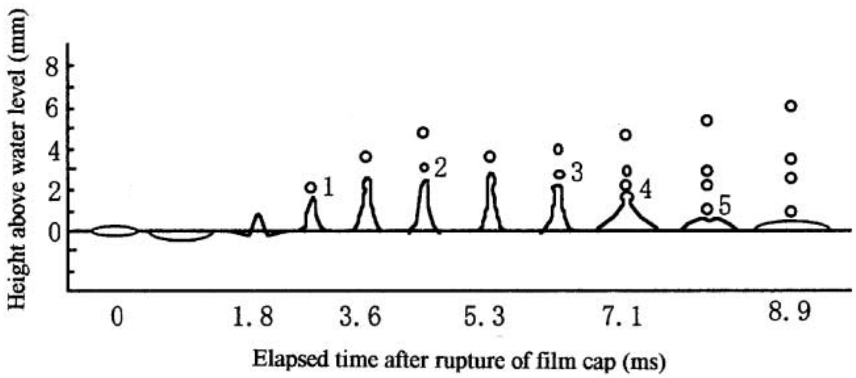

Figure 4.7 Bubble bursting phenomenon captured by Sugimoto and Higayashima

In Figure 4.7, it can be seen that 0 ms is when the bubble reaches its equilibrium position at the surface. After the bubble reaches the surface, the bubble cap disappear, leaving a bubble cavity that is tend to close up and producing liquid jet. The series of events can be captured by using FLUENT 12.0. Sugimoto and Higayashima do not show any formation of film droplets but jet droplets are visible to see. However, bubble that is used by Sugimoto and Higayashima is different with bubble in simulation. This comparison is made to see only on bubble bursting phenomenon. Thus, bubble bursting phenomenon is similar for all size of bubble. As the ejection of jet droplets is depending on the parent bubble size, thus, the results of no jet droplets can be due to coarse mesh or large bubble size.

4.2. Effect of Initial Bubble Diameter to Bubble Bursting

In order to observe the effect of initial bubble diameter on bubble bursting phenomenon, the case is run for two different sizes of bubble diameter which are 9.3 mm and 11.5 mm. The surface tension is held constant at 1.2 N/m. Figure 4.8 below shows the comparison on the initial condition of both cases.

Initial Bubble Diameter at t = 0 s	
9.3 mm	**11.5 mm**
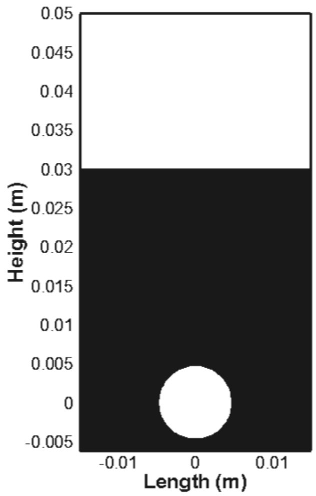	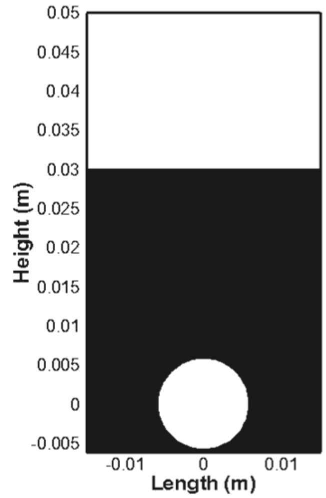

Figure 4.8 Initial condition for 9.3 mm and 11.5 mm diameter of bubble

It can be seen that the path for bubble to rise and reach the surface is the same. For comparison, observations are made at every main events. Position and time for each bubble to reach the surface, bubble cap completely disappear and highest liquid jet production are shown in Figure 4.9, 4.10 and 4.11, respectively.

Initial Bubble Diameter	
9.3 mm	**11.5 mm**
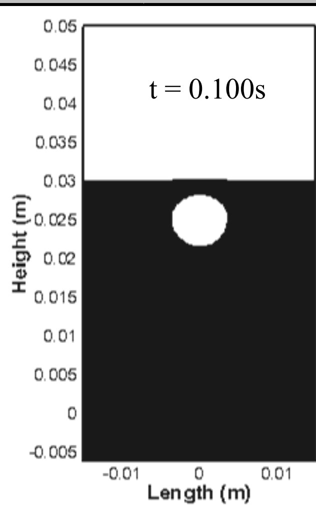	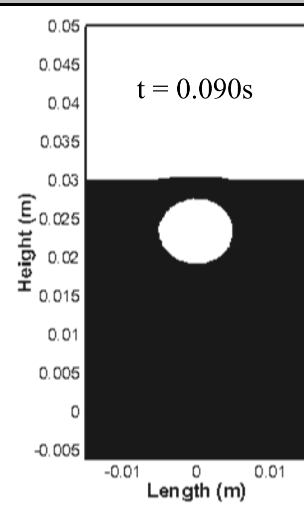

Figure 4.9 Time for bubble reaches the surface for different bubble size

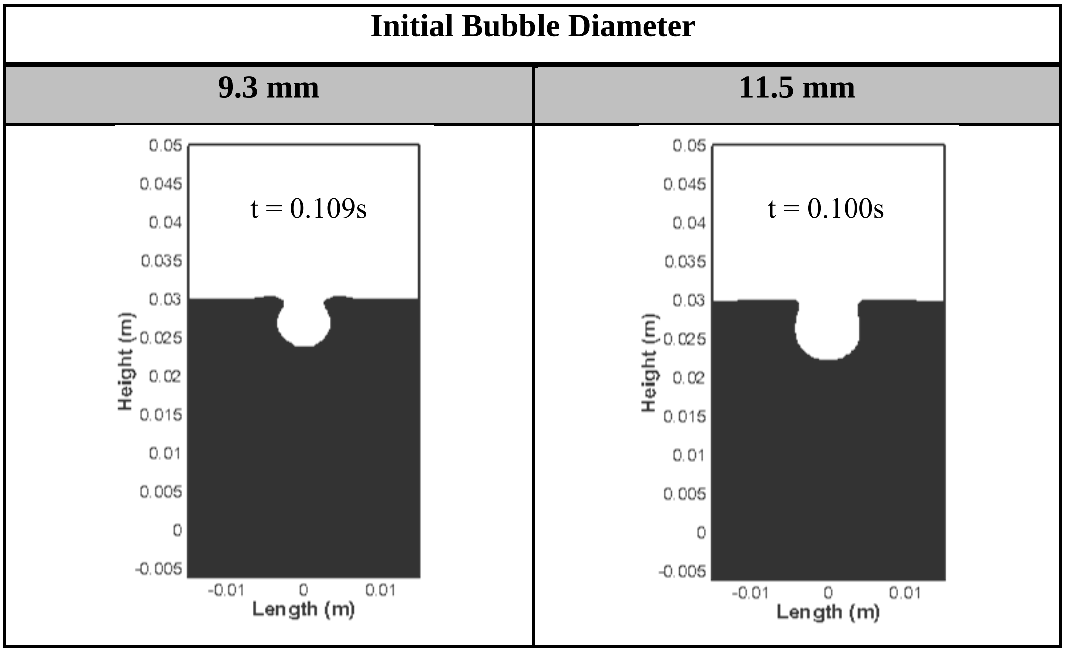

Figure 4.10 Time for bubble cap to completely disappear for different bubble size

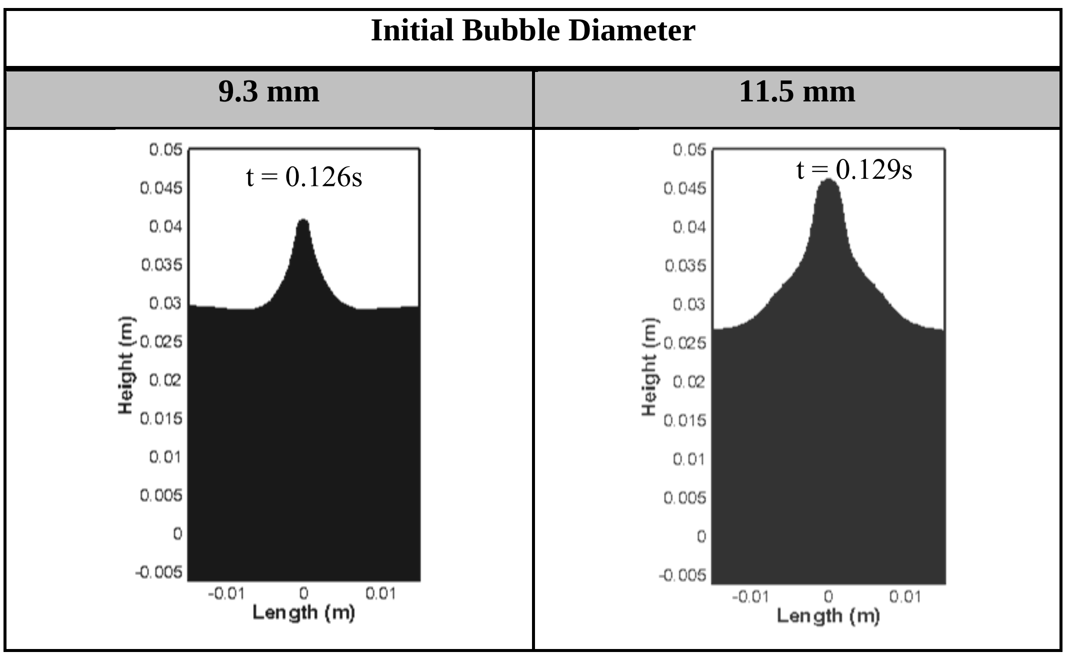

Figure 4.11 Time for highest liquid jet for different bubble size

From Figure 4.9, bubble with 11.5 mm of diameter reaches the surface before the smaller one and this indicates that bigger bubble rises faster than small bubble. According to Krishna and colleagues [17] rise velocity of bubbles is describe by Davies –Taylor relation with some introduction of scale factor, SF (refer Equation 14).

$$V_b^0 = 0.71\sqrt{gd_b}\,(SF) \quad (14)$$

Scale factor which is derived by Collins[18] is depending on the range of the ratio of bubble's diameter to column's diameter. As in this case, the scale factor is the same as they lay within the same range. Based on Equation 14, the relation between bubble rise velocity and bubble's diameter is directly proportional, thus drawing a conclusion on larger bubble rise faster than small bubble like shown in Figure 4.9.

In Figure 4.10, bubble with 9.3 mm of diameter needs 9 ms for its film to completely disappear. While bubble with 11.5 mm of diameter needs 10 ms. It also can be observed that the bubble cavity is larger for larger bubble. This different in cavity size is the main reason for difference in liquid jet. As it can be seen in Figure 4.11, liquid jet produced by bubble with 11.5 mm of diameter is higher than 9.3 mm. The height of liquid jet is depending on the area of bubble cavity as the bigger area of bubble cavityAs no droplet can be found in both cases, thus no conclusion can be made to direct relate between bubble size and formation of droplets.

CHAPTER 5: CONCLUSIONS

Bubble bursting phenomenon that is captured by using FLUENT 12.0 in this study is similar compare to results that are gathered from existing experimental data. Simulation on bubble bursting has been done to see the relationship between bubble bursting phenomenon with bubble diameter and surface tension. For bubble diameter, the simulation has been done on two different bubble diameters which are 9.3 mm and 11.5 mm, while surface tensions are determined to be 1.2 N/m and 1.4 N/m. These values are determined from the validation cases that are used for comparison. Bubble bursting phenomenon that are captured are similar for each different case. It can be seen generally Bubble bursting phenomenon consists of series of main events which are formation one single hole on bubble film, bubble film breakage and liquid jet production. All of these events can be captured by using FLUENT 12.0 and agree with literature review.

However, film droplets and jet droplets that are expected to form cannot be seen in all the cases making it difficult to distinguish the difference on the effects of the key parameters. This is expected due to coarse meshes that are not fine enough to capture the droplets. Finer mesh is highly recommended in order to capture the droplets.

REFERENCES

1. Guézennec, A.-G., et al., (2005). Dust formation in Electric Arc Furnace: Birth of the particles, *Powder Technology*, **157,1-3**, pp. 2-11.
2. Han, Z. and L. Holappa, (2003). Bubble bursting phenomenon in Gas/Metal/Slag systems, *Metallurgical and Materials Transactions B*, **34,5**, pp. 525-532.
3. R. Tsujino, M.H., T. Ohno, N. Ishiwata and T.Inoshita, (1898). Mechanism of Dust Generation in a Converter with Minimum Slag, *The Iron and Steel Institute of Japan*, **29,4**, pp. 291-99.
4. Kuo, H.-W., J.-S. Lai, and T.-I. Lin, (1997). Nasal septum lesions and lung function in workers exposed to chromic acid in electroplating factories, *International Archives of Occupational and Environmental Health*, **70,4**, pp. 272-276.
5. Howell, P.D., (1999). The draining of a two-dimensional bubble, *Journal of Engineering Mathematics*, **35**, pp. 251-272.
6. Dey, D., Boulton-Stone, J. M., Emery, A. N., and Blake, J. R., (1997). Experimental comparisons with a numerical model of surfactant effects on the burst of a single bubble, *Chemical Engineering Science*, **52,16**, pp. 2769-2783.
7. Reinke, N., Voßnacke, A., Schütz, W., Koch, M. K., and Unger, H., (2001). Aerosol Generation by Bubble Collapse at Ocean Surfaces, *Water, Air, & Soil Pollution: Focus*, **1,5**, pp. 333-340.
8. A. G. Guézennec, J.C.H., F. Patisson, Ph. Sessiecq, J. P. Birat And D. Ablitzer, (2004). Dust Formation by Bubble-burst Phenomenon at the Surface of a Liquid Steel Bath.
9. Higashiyama, T.S.a.Y., (2001). Production of water drops and corona due to rupture of air bubbles at water surface under a positive dc electric field, *Journal of Electrostatics*, **53**, pp. 209–219.
10. Günther, A., S. Wälchli, and P.R. von Rohr, (2003). Droplet production from disintegrating bubbles at water surfaces. Single vs. multiple bubbles, *International Journal of Multiphase Flow*, **29,5**, pp. 795-811.

11. Boulton-Stone, J.M. and J.R. Blake, (1993). Gas bubbles bursting at a free surface, *Journal of Fluid Mechanics Digital Archive*, **254,-1**, pp. 437-466.

12. Sussman, M., et al., (1998). An improved level set method for incompressible two-phase flows, *Computers & Fluids*, **27,5-6**, pp. 663-680.

13. Georgescu, S.-C., J.-L. Achard, and É. Canot, (2002). Jet drops ejection in bursting gas bubble processes, *European Journal of Mechanics - B/Fluids*, **21,2**, pp. 265-280.

14. Mostaghimi, N.A.J., *An Introduction to Computational Fluid Dynamics*, in *Fluid Flow Handbook*.

15. Vinay R. Gopala, B.G.M.v.W., (2008). Volume of fluid methods for immiscible-fluid and free-surface flows, *Chemical Engineering Journal 141*, pp. 204–221.

16. Johnston, H. *Bursting Bubbles Cascade on Camera*. 2010; Available from: http://physicsworld.com/cws/article/news/42898.

17. Krishna, R., et al., (1999). Rise velocity of a swarm of large gas bubbles in liquids, *Chemical Engineering Science*, **54,2**, pp. 171-183.

18. Collins, R., (1967). The effect of a containing cylindrical boundary on the velocity of a large gas bubble in a liquid, *Journal of Fluid Mechanics*,**28**, pp. 97-112.